JOURNAL OF SOLID STATE CHEMISTRY 97, 65–73 (1992)

Electric Transport Properties of the β-LnNb$_3$O$_9$ Phases (Ln = La, Ce, Pr, and Nd)

EMILIO ORGAZ[1] AND ALFONSO HUANOSTA

Instituto de Investigaciones en Materiales, Universidad Nacional Autónoma de México, AP 70-360, CP 04510, Mexico, Distrito Federal, Mexico

Received June 11, 1991; in revised form September 4, 1991

The electric properties of the cation deficient perovskites of the formula β-LnNb$_3$O$_9$, where Ln is La, Ce, Pr, or Nd, were investigated by means of the impedance spectroscopy technique. The electric conductivity behavior of the β-LnNb$_3$O$_9$ phases shows a clear trend in the activation energy for electric transport that can be easily correlated to the small changes in the unit cell volume. The β-LnNb$_3$O$_9$ series shows similar dielectric loss behavior, with the exception of the β-CeNb$_3$O$_9$ phase. The β-CeNb$_3$O$_9$ compound shows an electronic contribution to the electric conduction which seems to be present in the entire range of temperatures investigated.

Introduction

Niobium pentaoxide reacts with rare earth oxides to produce compounds with the formula β-LnNb$_3$O$_9$ where Ln is La, Ce, Pr, or Nd (*1*). The β-LnNb$_3$O$_9$ phases present the orthorhombic structure (P_{mmm}) shown in Fig. 1. This structure was refined from X-ray diffraction on single crystals (*1*) and it can be described as the stacking of two cubic perovskite units where $\frac{4}{3}$ of the lanthanide sites are vacant. The formula per unit cell is then $Ln_{2/3}$Nb$_2$O$_6$. A structural distortion of the NbO$_6$ units in the c direction was also detected, giving four crystallographic types of oxygens.

Torardi, Brixner, and Foris (*2*) obtained, by hydrothermal methods, a low-temperature form of LaNb$_3$O$_9$ named the α-phase. It consists of an ordered monoclinic structure, which transforms upon heating to the more stable β-phase at 1323–1373 K. The β-phase structure is retained on cooling to ambient temperature. Luminescence investigations in both phases were carried out by Verhaar *et al.* (*3*). The spectrum of the β-phase shows broad lines, probably due to the disorder in the lanthanide sites. It was also determined, by infrared spectroscopy, that the NbO$_6$ units are discrete and highly distorted (*3*).

The electrical properties of this cation-deficient structure have been investigated looking for the possibility of ionic conduction due to the numerous vacant sites. Doped niobates with the formula Li$_x$ $Ln_{2/3}$Nb$_{2-x}$Ti$_x$O$_6$ (Ln = La, Nd, with $x < 0.20$) were investigated by Latie *et al.* (*4*). In this solid solution, the replacement of Nb^{+5} by Ti^{+4} + Li^{+1} preserves the electroneutrality of the compound without change of the charge state of the niobium atoms. The authors found that the electrical con-

[1] Permanent address: UA-446, bât, 415, Université de Paris-Sud, 91405 Orsay-Cedex, France.

0022-4596/92 $3.00

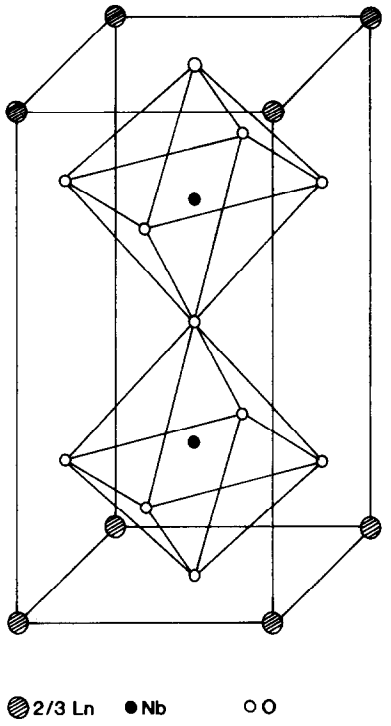

FIG. 1. Unit cell of the β-LnNb$_3$O$_9$ structure (details described in the text).

ductivity (ionic in nature) is increased by Li doping. Their ^{7}Li NMR experiments did not give conclusive evidence regarding the dimensionality of the transport process.

The same group (*5*) produced phases with the formula Li$_x$$Ln_{2/3}Nb_2O_6$ (Ln = La, Nd) by chemical and electrochemical Li-intercalation techniques. They were able to obtain a single phase with lithium content as high as $x \cong 1.6$. Several experiments were carried out in these compounds. The main findings were that the electrical conductivity is increased by two orders of magnitude when the Li content passes from $x = 0$ to $x = 1.6$ at 500 K. ESR experiments in samples with low Li content showed the existence of niobium in the 4^+ state. For the undoped material, the gap energy determined by diffuse reflectance in the UV and visible region was 3.1 eV, while constant absorption in the full wavelength region was observed in compounds with $x \neq 0$. According with the two last observations, it was proposed that the conduction in the Li-intercalated compounds is mainly due to electron hopping process.

The β-LaNb$_3$O$_9$ phase was recently investigated by George and Virkar (*6*), who found a mixed iono-electronic conduction mechanism as a function of temperature. Below 850 K, the stoichiometric β-La$_{2/3}$Nb$_2$O$_6$ phase shows ionic conduction, while above 850 K (in air), the β-phase is chemically reduced. Oxygen vacancies are then produced and mobile electrons compete with the ionic conductivity. A clear change in the activation energy for the conduction processes was observed; E_a changes from 0.19 to 1.58 eV. In this research, it has been confirmed that the defect equation (*1*) (in the Kröger notation (*7*))

$$O_{\text{lattice}} \rightarrow V_a^{**} + 2e^- + \tfrac{1}{2} O_{2(g)} \qquad (1)$$

is appropriate to describe the n-type conduction. In this work the $p_{O_2}^{1/6}$-dependence of the electrical conductivity was verified. The ionic conduction is due to the lanthanum transport, a large and highly charged carrier.

The impedance spectroscopy technique is an experimental method widely used to determine the behavior of the dielectric materials. This technique permits a clear separation of the different contributions (bulk, grain boundaries, second phases, etc.) to the electric conductivity by modeling the material as an RC-circuit (*8*).

In this paper we extend the research on the β-LnNb$_3$O$_9$ compounds by a complete impedance spectroscopic characterization including the phases with Ln = La, Ce, Pr, and Nd. This paper is organized as follows. In the second part, we present the experimental aspects, sample preparation, X-ray and TGA controls, and the frequency-dependent impedance measurements. Next, we present the experimental results and the discussion of the electrical conductivity

TABLE I

LATTICE PARAMETERS AND CELL VOLUME (IN Å AND Å^3)

	$\bar{a}$	$\bar{b}$	$\bar{c}$	$\bar{V}$
$LaNb_3O_9$	3.911(8)	3.911(8)	7.92(7)	121.1(4)
$CeNb_3O_9$	3.903(8)	3.919(8)	7.87(7)	120.4(7)
$PrNb_3O_9$	3.881(8)	3.910(8)	7.85(7)	119.3(4)
$NdNb_3O_9$	3.882(8)	3.904(7)	7.82(7)	118.6(5)

data, and then we describe the dielectric behavior. Finally, we point out the particular electric behavior of the β-$CeNb_3O_9$ phase.

Experimental

Sample Preparation

β-$LnNb_3O_9$ samples were prepared by mixing with acetone in an agate mortar, La_2O_3, CeO_2, Pr_6O_{11}, or Nd_2O_3 with Nb_2O_5, in the molar ratios to obtain the β-$Ln_{2/3}Nb_2O_6$ phases. La_2O_3, CeO_2, and Nb_2O_5 were obtained from Anderson Physics Laboratories, while Pr_6O_{11} and Nd_2O_3 came from Reacton. The purity of these chemicals (99.99%) is adequate for the purpose of this investigation. The oxide mixtures were sintered thrice at 1573 K for 48 hr in air. All the samples were annealed in air at 573 K for at least 72 hr.

X-ray and TGA Controls

X-ray powder diffraction data were obtained by using Ni-filtered Cu$K\alpha$ radiation. The samples showed single phases of the orthorhombic structure. No second phases were detected. The lattice parameters and cell volume, shown in Table I, are in good agreement with earlier studies (*1, 2*). Thermogravimetric analysis (TGA) was carried out in flowing air at 2 K/min. The samples were thermally stabilized for 6hr at 673 K inside the TGA cell. The characteristic temperatures at which the β-$LnNb_3O_9$ phases lose oxygen were determined and were about 718 K.

Electric Transport Measurements

We prepared flat cylindric samples of β-$Ln_{2/3}Nb_2O_6$ (13 mm in diameter and around 1 mm in thickness). The electrodes consisted of gold films attached with electronic grade gold paste. In order to obtain good ohmic contact, the samples were fired at 873 K for 60 min. The samples were then re-annealed in air for 3 days at 573 K to restore the maximum oxygen content. We placed the samples in a regulated vertical furnace where the temperature is known within ± 1 K. The complex impedance was determined as a function of frequency (5 Hz to 13 MHz) at each temperature using an impedance analyzer (HP-4192A).

The output data were analyzed in the complex impedance plane. The resistance values were transformed to electrical conductivity by considering the sample geometry. No further corrections were made. In our experimental conditions, the conductivity limit detection was $10^{-7.5}$ $(\Omega\ \text{cm})^{-1}$. This value implies a lower limit in the temperature range to be investigated. At high electrical conductivity values ($\sigma > 10^{-3}$ $(\Omega\ \text{cm})^{-1}$), we also collected experimental data of the dc resistance of the samples. In these measurements reasonable agreement was found between the ac and dc technique.

Results and Discussion

Conductivity Results

In Figs. 2–5 we show the experimental results of the electrical conductivity in the standard representation log σ vs $1/T$ for the four compounds studied. We calculated the activation energies for electric transport (E_a) according to the relation

$$\sigma = \sigma_0/T \exp(E_a/k_B T), \qquad (2)$$

where σ is the electric conductivity, T the

TABLE II
ACTIVATION ENERGIES

	Temperature range (K)	E_a (eV)
$LaNb_3O_9$	1000–1173	1.24
	473– 713	0.38
$CeNb_3O_9$	335–1173	0.38
$PrNb_3O_9$	473–1000	0.43
$NdNb_3O_9$	473–1073	0.48

absolute temperature, and k_B the Boltzmann constant. The calculated E_a values estimated in the linear range are listed in Table II.

Comparing our results of β-$LaNb_3O_9$ (Fig. 2) with those of George and Virkar (*6*), we find that the overall behavior of σ vs T is similar. The temperature at which the change in the activation energy is present remains essentially the same in both investigations. Nevertheless, differences in the activation energies and the order of magnitude of the conductivity are evident. We found that σ is two orders of magnitude higher than the results reported by George and Virkar (*6*). Nadiri, Le Flem, and Delmas (*5*) mentioned that the σ value of β-$LaNb_3O_9$ at room temperature is lower than 10^{-10} $(\Omega\ cm)^{-1}$ (four probe, dc-technique). Extrapolating the conductivity values of George and Virkar (*6*) to room temperature, we found

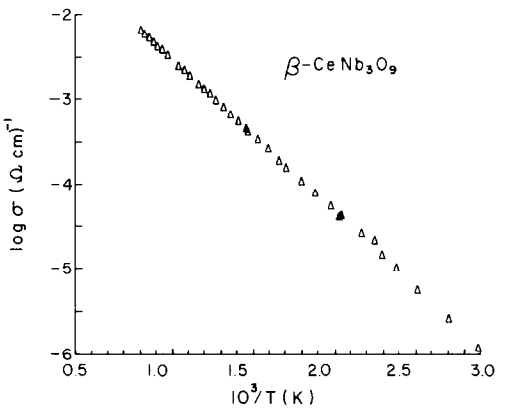

FIG. 3. Log σ $(\Omega\ cm)^{-1}$ vs $10^3/T$(K) results of the β-$CeNb_3O_9$ phase. Open symbols represent measurements taken after thermal equilibration for 2 or 3 hr. Closed symbols represent measurements taken after overnight equilibration.

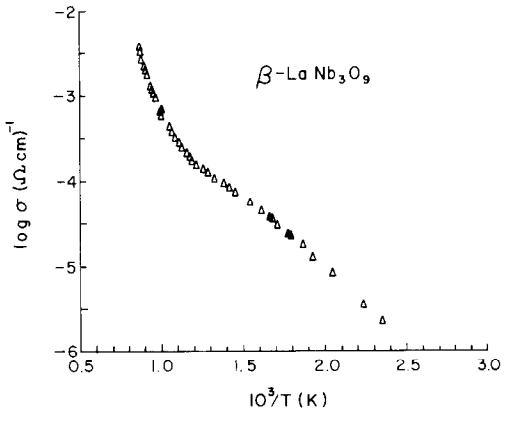

FIG. 2. Log σ $(\Omega\ cm)^{-1}$ vs $10^3/T$(K) results of the β-$LaNb_3O_9$ phase. Open symbols represent measurements taken after thermal equilibration for 2 or 3 hr. Closed symbols represent measurements taken after overnight equilibration.

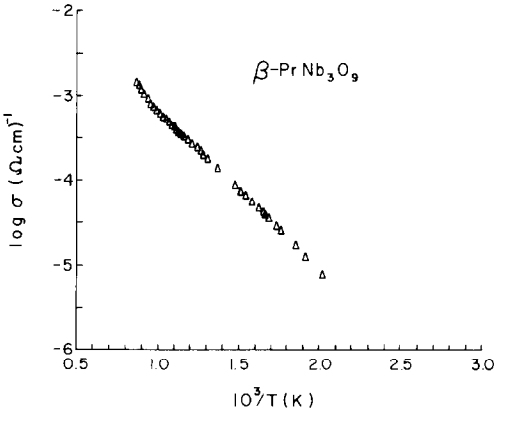

FIG. 4. Log σ $(\Omega\ cm)^{-1}$ vs $10^3/T$(K) results of the β-$PrNb_3O_9$ phase. Open symbols represent measurements taken after thermal equilibration for 2 or 3 hr. Closed symbols represent measurements taken after overnight equilibration.

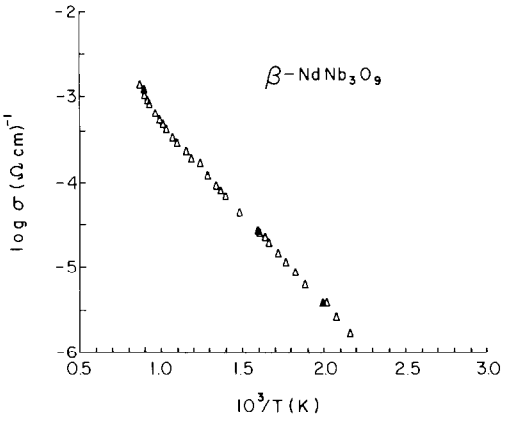

FIG. 5. Log σ (Ω cm)$^{-1}$ vs $10^3/T$(K) results of the β-NdNb$_3$O$_9$ phase. Open symbols represent measurements taken after thermal equilibration for 2 or 3 hr. Closed symbols represent measurements taken after overnight equilibration.

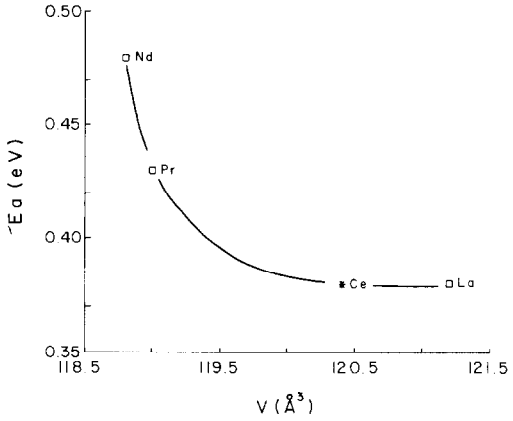

FIG. 6. Plot of the activation energy E_a (eV) vs the cell volume V (Å^3). Note the increase of the activation energy when the volume cell diminishes. The solid line is to guide the eye.

that σ is two orders of magnitude higher than this value (ac-technique at 1kHz).

Referring to Figs. 2–5, it is interesting to note the behavior of the electrical conductivity in this series. For temperatures below 700 K, the β-LnNb$_3$O$_9$ (Ln = La, Pr, Nd) phases show similar conductivity values with activation energies close to 0.40 eV. This result could be interpreted as a test of self-consistency of our experimental data. The structure of these phases show small variations in the cell parameters from one lanthanide to other. These small structural differences are not enough to produce radical changes in $\sigma = \sigma(T)$ and the values of E_a. The β-CeNb$_3$O$_9$ phase shows a different behavior, and it is discussed below. Figure 6 shows the trend of the activation energies with the cell volume for the β-LnNb$_3$O$_9$ phases (Ln = La, Ce, Pr, Nd). We included in this plot the E_a value of the β-CeNb$_3$O$_9$ compound, which conforms to the general trend. The behavior shown in Fig. 6 is qualitatively in agreement with an ionic conduction mechanism; the potential energy barrier for ionic transport increases when the cell volume decreases. Two sublattices are available for La transport, one involving vacancies in the (0,0,1) plane and a second in the vacant lanthanide sites at the (0,0,2) plane. Thus, ionic conduction can be obtained in each of both sublattices (2D conduction), or by ion jumps from one sublattice to the other (3D conduction).

In Fig. 7, we present the complex imped-

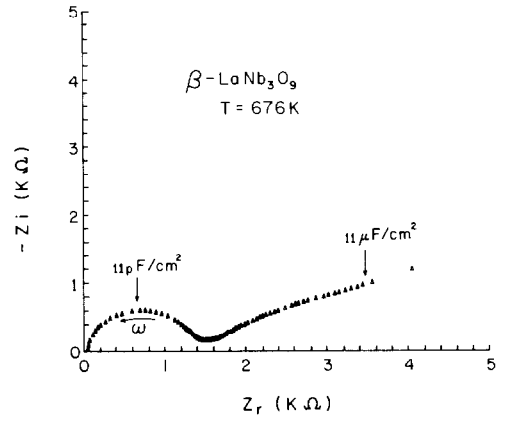

FIG. 7. Complex impedance plot for the β-LaNb$_3$O$_9$ phase at 676 K. The arrow shows the way of the frequency (ω) scan. The values of capacitance at the resonance condition are shown.

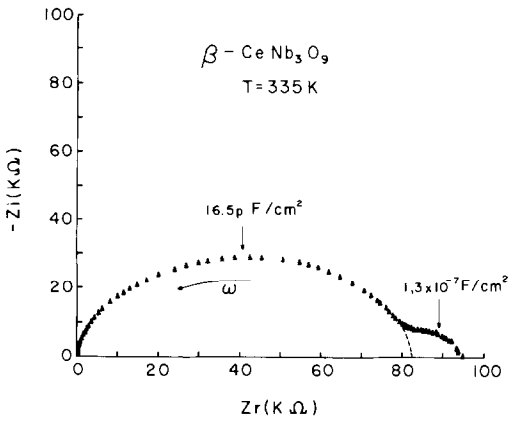

FIG. 8. Complex impedance plot for the β-$CeNb_3O_9$ phase at 335 K. The arrow shows the way of the frequency (ω) scan. The values of capacitance at the resonance condition are shown.

ance plot for the lanthanum-based compound at $T = 676$ K. We found one characteristic semicircle representing the bulk behavior of the sample. At the loss peak frequency ($\omega RC = 1$), we derived a capacitance of 11 pF/cm^2. At lower frequencies it appears as a well known behavior (*8*) attributed to the electrode-sample polarization (high capacitance $\cong 11$ μF/cm^2). This effect is a common feature of ionic conductors. The shape of the plot in Fig. 7 is representative of the compounds β-$Ln Nb_3O_9$ (Ln = La, Pr, Nd) at low temperatures. Above the temperature for vacancies creation, the semicircle is not well defined, due to the high conductivity of the material compared to the electric properties of the experimental setup.

In the case of β-$CeNb_3O_9$, we observe that the $\sigma = \sigma(T)$ values are one order of magnitude higher than those of the β-$Ln Nb_3O_9$ (Ln = La, Pr, Nd). The change in the activation energy at 850 K, in the β-$LnNb_3O_9$ and due to the creation of oxygen vacancies, is absent in the cerium-based phase. Figure 8 presents the complex impedance plot for the Cerium-based compound at $T = 335$ K. The characteristic spike present at low temperature and frequencies for the other β-$LnNb_3O_9$ compounds is not present here. Instead of this, a second semicircle appears. The capacitances for the two peaks are 16.5 pF/cm^2 and 1.3×10^{-7} F/cm^2. The last value is commonly attributed to a surface layer formed between the material and the electrodes. Again, when the temperature is raised the semicircles in the Fig. 8 disappear due to the high conductivity of the sample.

Dielectric Behavior

The dielectric behavior of these materials is discussed with the aid of two representations. In the first, we calculated the relaxation time as a function of the temperature. In the second, we investigated the behavior of the impedance spectroscopic plots Im Z^* vs log f (the imaginary part of the impedance as a function of the frequence).

The relaxation time was calculated directly from the complex impedance plots as $\tau = RC = \omega_{max}^{-1}$, at each temperature (not shown). We also calculate the theoretical semicircle and the corresponding calculated relaxation time in the Debye approximation. The relaxation time is the required time to reach equilibria; it is a characteristic parameter of the thermally activated ionic hopping. It is well known that the departures of the Debye behavior contains informations about dissipative phenomena in the dipole re-orientation mechanism and dipole–dipole correlations.

Our experimental results show Arrhenius-like behavior at low temperatures in the β-$Ln Nb_3O_9$ series. At high temperatures their departure from the Arrhenius-like behavior is significant. The strong changes in the electric properties when the temperature is increased make these materials good conductors and, as we described above, the semicircles are not well determined. The parameters of the Arrhenius fit and the departure of the Debye model are summarized in the Table III.

TABLE III

RELAXATION TIME

	E_{exp}	E_{Debye}	$\tau_{0\,exp}$	$\tau_{0\,Debye}$	$\Delta\tau_0$
$LaNb_3O_9$	0.42	0.33	7.36	59.37	52.01
$CeNb_3O_9$	0.37	0.36	1.99	3.93	1.94
$PrNb_3O_9$	0.43	0.47	6.37	2.24	−4.12
$NdNb_3O_9$	0.45	0.40	24.64	92.04	67.40

Note. E is the activation energy in eV, τ_0 is the pre-exponential relaxation time expressed in 10^{11} Hz, exp holds for the experimental data, Debye for the calculated values, and $\Delta\tau_0$ is the difference between theory and experiment.

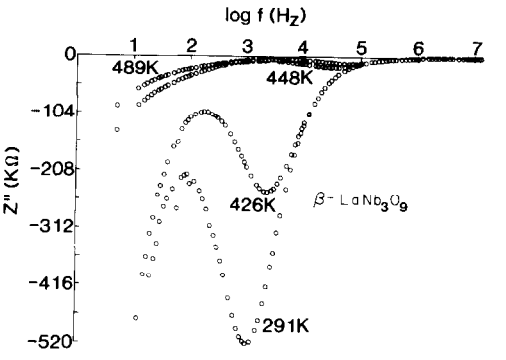

FIG. 10. Impedance spectroscopic plot Im Z^* vs log f for the β-$LaNb_3O_9$ for different temperatures.

The impedance spectroscopic plot for β-$LaNb_3O_9$ at 354 K is shown in Fig. 9. In this plot we show the real (z') and imaginary (z'') parts of the impedance as a function of frequency. We calculated the classical Debye behavior using the center of the semicircle of the complex impedance data and correcting by the departure from the Im $Z^* = 0$ axis (*9*). The theoretical curves only show the bulk behavior. The details at low frequencies are not considered in this simple model.

In Figs. 10–13, we show the impedance spectroscopic plots for the β-LnNb$_3$O$_9$ series at different temperatures. This set of plots describes the evolution of the dielectric relaxation as a function of temperature an frequency. The dielectric loss peak behavior reflects similar relaxation mechanisms in the β-LnNb$_3$O$_9$ series. The behavior at low frequencies is divergent for the β-LnNb$_3$O$_9$ (Ln = La, Pr, Nd), while for the Ce-based compound, the absolute value of Im Z^* decreases when the frequency diminishes. We attribute this behavior to the presence of electronic conduction in this material. The values of Im Z^* at the loss peak are systematically equal to $R_b/2$ (where R_b is the bulk resistance of the sample).

Electronic Contribution to the β-$CeNb_3O_9$ Electric Tranport

An interesting consideration derived from our measurements on the β-$CeNb_3O_9$ com-

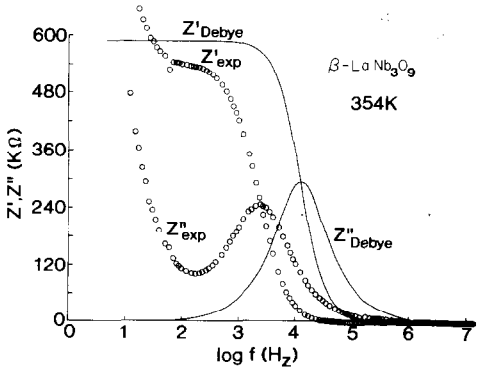

FIG. 9. Impedance spectroscopic plot Re Z^* vs log f and Im Z^* vs log f for the β-$LaNb_3O_9$ at 354 K.

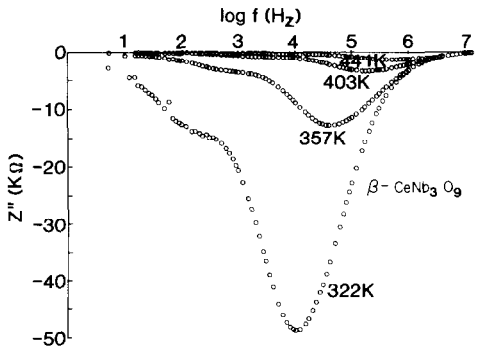

FIG. 11. Impedance spectroscopic plot Im Z^* vs log f for the β-$CeNb_3O_9$ for different temperatures.

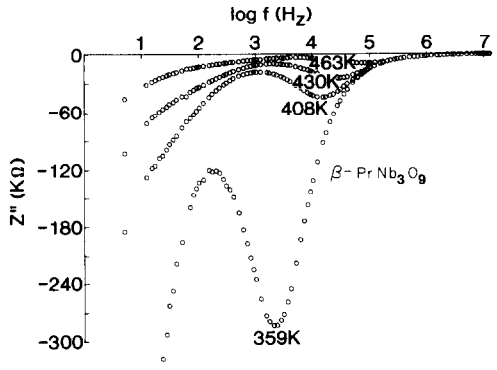

FIG. 12. Impedance spectroscopic plot Im Z^* vs log f for the β-$PrNb_3O_9$ for different temperatures.

pound is that the electric transport in this phase probably has a large electronic component over the entire range of temperatures investigated. The niobium atoms in the β-$LnNb_3O_9$ are present in the 5^+ state, while the charge state of the lanthanides is 3^+. Nevertheless, as we mentioned in the introduction, by suitable doping (Li-intercalation or by introducing oxygen vacancies) it is possible to reduce niobium atoms to the Nb^{+4} state in β-$LnNb_3O_9$ (Ln = La and Nd) (*4–6*). It is well known that the lanthanides are frequently present in a mixed valence state in a large number of compounds (*10*). It is plausible that a charge transfer from cerium to niobium atoms produce d-niobium band localized electrons. Considering the chemical formula $Ce_{2/3}^{q}Nb_2O_{6-y}$, the number of electrons in the d band is $n_d = y + q/3 - 1$. In the last equation, y is the amount of oxygen non-stoichiometry and q is the charge state of Ce in this compound. A hopping mechanism should contribute to the overall conductivity in the temperature range investigated. This assertion is supported by our recent results of lithium intercalation of β-$CeNb_3O_9$. We found a very significant increase of the electrical conductivity when lithium was incorporated to the structure. As an example, the electrical conductivity of the $Li_xCeNb_3O_9$ phase ($x \cong 0.3$) is of the order of 10 $(\Omega\ cm)^{-1}$, seven orders of magnitude higher than in the case of β-$CeNb_3O_9$ at the same temperature. This dramatic change in the electric conductivity was not observed in the β-$LnNb_3O_9$ (Ln = La and Nd) previously investigated (*5*). The results regarding the β-$Li_xCeNb_3O_9$ phase will be reported elsewhere (*11*).

From the present results, it is clear that more investigations on the electronic structure of these phases and the role of the oxygen stoichiometry on the electric properties are necessary.

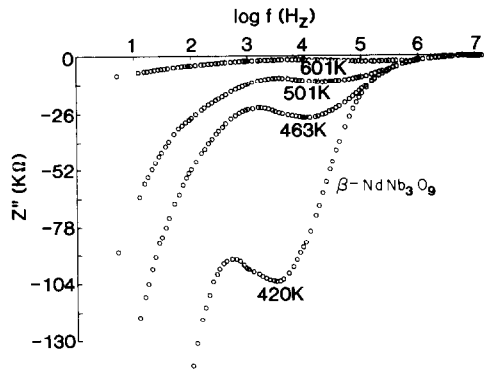

FIG. 13. Impedance spectroscopic plot Im Z^* vs log f for the β-$NdNb_3O_9$ for different temperatures.

Acknowledgments

This research was supported by the Universidad Nacional Autónoma de México under Grant DGAPA-IN-104291 and by the Programa Universitario de Superconductores de alta Temperatura de Transición (PUSCATT).

References

1. P. IYER AND A. J. SMITH, *Acta Crystallogr.* **23,** 740 (1967).
2. C. C. TORARDI, L. H. BRIXNER, AND C. M. FORIS, *J. Solid State Chem.* **58,** 204 (1985).
3. H. C. G. VERHAAR, H. DONKER, G. J. DIRKSEN, M. J. J. LAMMERS, G. BLASSE, C. C. TORARDI, AND L. H. BRIXNER, *J. Solid State Chem.* **60,** 20 (1985).
4. L. LATIE, G. VILLENEUVE, D. CONTE, AND G. LE FLEM, *J. Solid State Chem.* **51,** 293 (1984).

5. A. NADIRI, G. LE FLEM, AND C. DELMAS, *J. Solid State Chem.* **73,** 338 (1988).
6. A. M. GEORGE AND A. N. VIRKAR, *J. Phys. Chem. Solids.* **49,** 743 (1988).
7. F. A. KRÖGER "The Chemistry of Imperfect Crystals," Vol. 2, North-Holland, Amsterdam (1974).
8. J. ROSS MACDONALD, "Impedance Spectroscopy," Wiley, Chichester (1987); D. C. Sinclair and A. R. West, *J. Appl. Phys.* **66,** 3850 (1989); J. T. S. Irvine, D. C. Sinclair, and A. R. West, *Adv. Mater.* **2,** 132 (1990).
9. K. S. COLE AND R. N. COLE, *J. Chem. Phys.* **9,** 341 (1941); S. P. S. Badwal, *in* "Proceedings, International Seminar, Solid State Ionic Devices" (B. V. R. Chowdari and S. Radhakrishna, Eds.), p. 165, World Scientific, Singapore (1988); K. Jonscher, *J. Mater. Sci.* **24,** 372 (1989).
10. K. A. GSCHNEIDER, JR., L. EYRING, AND S. HÜFNER (EDS.), "Handbook of the Physics and Chemistry of Rare Earths, Vol. 10: High Energy Spectroscopy," North-Holland, Amsterdam (1987).
11. E. ORGAZ, G. TAVIZÓN, AND G. FERRER, submitted for publication.